Correlation between the extraordinary Hall constant and electrical resistivity minima in Co-rich metallic glasses

A. K. Majumdar* and P. K. Khatua

Department of Physics, Indian Institute of Technology, Kanpur 208016, Uttar Pradesh, India

K. D. D. Rathnayaka and D. G. Naugle

Department of Physics, Texas A&M University, College Station, Texas 77843-4242, USA

The Hall effect has been studied in some Co-rich ferromagnetic metallic glasses which show resistivity (ρ) minima at low temperatures. It is found that the extraordinary Hall constant (R_s) shows a corresponding minimum. The scaling relation $R_s \sim \rho^n$ holds with $n \simeq 2$ showing the dominance of quantum transport in these high-resistive disordered systems. The temperature dependences of magnetization and electrical resistivity are also interpreted in terms of existing theories.

I. INTRODUCTION

The Hall resistivity (ρ_H) in a crystalline ferromagnet is, for $T \ll T_c$, given by[1]

$$\rho_H = R_0 B + \mu_0 R_s M_s, \qquad (1)$$

where B is the magnetic induction and μ_0 is the permeability of free space. The Lorentz force acting on the charge carriers is responsible for the first term where R_0 is called the "ordinary Hall constant." This term is present in nonmagnetic materials as well. The second term, characteristic of a ferromagnet, depends on the saturation magnetization M_s while R_s is known as the "extraordinary" or the "spontaneous" Hall constant. In Eq. (1) R_0 and R_s have the same units of $\Omega m/T$ in SI. Two different mechanisms are responsible for R_s.

A. Nonclassical transport

It has been shown[1] that whenever the dimensionless parameter $\hbar / \tau E_F$, where τ is the electron relaxation time and E_F is the Fermi energy, becomes large, the classical Boltzmann equation does not hold and nonclassical terms begin to dominate. Karplus and Luttinger[2] and later on Luttinger,[3] using a quantum transport theory, were the first to predict that R_s is proportional to ρ^2, where ρ is the electrical resistivity. Due to the spin-orbit interaction present in a ferromagnet, the symmetry of the problem is low and there is a nonzero transverse electric field which gives rise to a Hall voltage. The above theories are quite complicated and involved. However, later on Berger[4] gave an intuitive picture of the physical mechanisms responsible for the Hall effect in concentrated ferromagnetic alloys and high temperatures. He proposed that an electron undergoes a discontinuous and finite "side jump" at every scattering by impurities or phonons. This also leads to the equation

$$R_S = b\rho^2. \qquad (2)$$

Both approaches,[3,4] by the way, predict that b in Eq. (2) is independent of the nature of the scatterer.

B. Asymmetric scattering

In the case of very dilute alloys at low temperatures the Boltzmann equation should be adequate. Here R_s is caused by "asymmetric scattering" of magnetized conduction electrons as proposed by Smit.[5] In the presence of a spin-orbit interaction there is a left-right asymmetry in the differential scattering cross-section about the $\vec{J} - \vec{M}$ plane where $\vec{J}$ is the current density. As a result charge carriers tend to pile up on one side of the sample producing a transverse electric field. Here

$$R_s = a\rho. \qquad (3)$$

The Hall effect in ferromagnetic metallic glasses has been reviewed at length by McGuire, Gambino, and O'handley[6] and Egami.[7] Equation (2) is found to be valid for R_s in Fe, Ni, and Co-based metallic glasses indicating the expected dominance of the side-jump mechanism in these high-resistive metallic glasses. The values of R_s in amorphous metals and alloys are, in general, much larger than those of their crystalline counterparts. This is a direct consequence of the much higher resistivity in the amorphous state. Also, here R_s has a weak temperature dependence because of the corresponding weak temperature dependence of the electrical resistivity since the disorder-induced resistivity dominates over the thermal contribution. Lachowicz[8] interpreted R_s in amorphous GdCo sputtered films in terms of two contributions, one coming from the skew scattering and the other from the nonclassical side-jump mechanism. However, Shiba *et al.*[9] explained R_s in amorphous Co-metal film by only the quantum mechanical side-jump mechanism ($R_s \sim \rho^2$). From the temperature dependence of both R_s and ρ, Ivkov *et al.*[10] obtained $R_s \sim \rho^2$ in a vast majority of Fe/Co/Ni-based amorphous alloys. Also, R_s is found to be positive for Fe and Co and negative for Ni-containing metallic glasses[1] at 300 K. However, most of the work reported till now is on those amorphous alloys where ρ monotonically increases with temperature and as does R_s. The motivation behind the present work is to track the scaling law $R_s \sim \rho^n$ where ρ shows a minimum at Tm, i.e., does R_s also show a minimum? How-

ever, we find that if R_sM_s decreases with temperature (as in the present case, but not necessarily so for other materials) by the same amount as M_s decreases with temperature, the change of R_s with temperature is very small (specially around the minimum) and becomes comparable to its experimental error. As a result a weak minimum is found in R_s near Tm in only two of the alloys. Also, we find that $n \simeq 2$ (side-jump mechanism) showing the dominance of the nonclassical mechanism for the origin of R_s.

II. EXPERIMENTAL DETAILS

The as-received metallic glass samples are in the form of ribbons, of typical width ~ 1 mm and thickness ~ 0.030 mm. The nominal compositions of the amorphous alloys are as follows.

  (i) Sample 1: $Fe_5Co_{50}Ni_{17}B_{16}Si_{12}$.
  (ii) Sample 2: $Fe_{7.8}Co_{31.2}Ni_{34}Cr_5B_{14}Si_8$.
  (iii) Sample 3: $Fe_{7.8}Co_{31.2}Ni_{29}Cr_{10}B_{14}Si_8$.
  (iv) Sample 4: $Fe_{7.8}Co_{31.2}Ni_{24}Mn_{15}B_{14}Si_8$.

They were prepared by melt quenching. The amorphous nature of the samples was checked by X-ray diffraction measurements using a Rich and Seifert Isodebyeflex 2002 diffractometer with a Cu target ($K_\alpha = 1.54$ Å). The results show broad peaks at low angles due to short-range order. There was no observable crystalline phase. The Hall resistivity (ρ_H) was measured using a standard 5-probe dc method for minimizing the resistive voltage arising from the misalignment of the Hall voltage probes. A voltage divider was made for each sample using two General Radio decade resistance boxes. The misalignment voltage was adjusted to within 1 μV or better at each temperature. The Hall resistivity was measured at 27 temperatures between 6 and 190 K and magnetic fields up to 3 T. The electrical resistivity in zero field was measured using a standard 4-probe dc setup from 4.2 to 200 K at every 1 K. The magnetization was measured in a magnetic field $\mu_0H = 1$ T using a Quantum Design superconducting quantum interference device (SQUID) magnetometer. T_c's of samples 1, 2, 3, and 4 are found to be $\simeq 395$, 386, 222, and 368 K, respectively.

III. RESULTS AND DISCUSSION

A. Hall effect

Figure 1 shows the Hall resistivity (ρ_H) against magnetic induction B for sample 4 at temperatures of 6, 49, 90, 131, and 188 K. In the Hall geometry the magnetic field is perpendicular to the sample plane and so the demagnetization factor $N \simeq 1$. Thus $\vec{B} = \mu_0[\vec{H}_{applied} + (1-N)\vec{M}_s] \simeq \mu_0\vec{H}_{applied}$. ρ_H shows the typical behavior of a ferromagnet for $T \ll T_c = 368$ K where ρ_H almost saturates beyond a certain B (here 1 T) and varies linearly with a slope R_0 and an intercept $\mu_0R_sM_s$. R_0 vs T for all the samples is plotted in Fig. 2 up to 190 K. The solid lines are just guides to the eye. R_0 is found to be positive over most of the temperature range and has a weak temperature dependence (except for sample 3) indicating minimal changes in the band structure in this temperature range. A sign change from negative to positive is observed below 30 K. R_0 has a much stronger temperature dependence
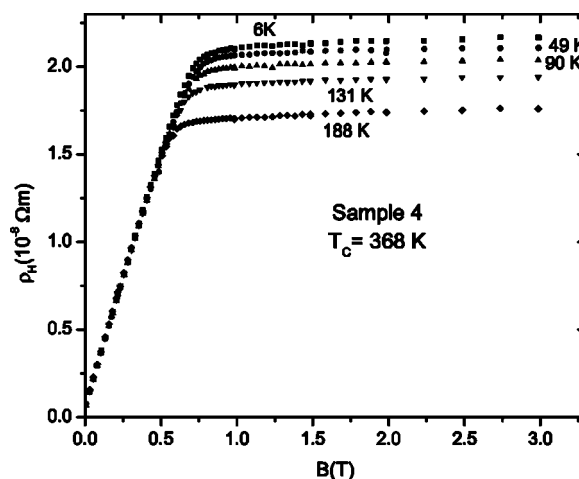

FIG. 1. Hall resistivity ρ_H vs magnetic induction B for sample 4 at 6, 49, 90, 131, and 188 K. They show typical behavior of a ferromagnet above 1T.

for sample 3. Whereas for the other three samples 190 K $\simeq T_c/2$, it is $\simeq T_c$ for sample 3. For ferromagnets the band splitting due to the exchange interaction disappears around T_c. This affects the carrier density as well as their conductivities making R_0 strongly temperature dependent around T_c as is the case with sample 3.

$\mu_0R_sM_s$ is plotted against temperature in Fig. 3 for all the samples. They show a weak decrease with temperature for $T < 50$ K. The solid lines are just guides to the eye. As expected for sample 3, $R_sM_s \rightarrow 0$ as $T \rightarrow T_c$ ($\simeq 222$ K). However, to extract $R_s(T)$ we use the SQUID data for M vs T which is shown in Fig. 4 at an external field of 1 T. Comparing Figs. 3 and 4 we observe that from 5 to 190 K, R_sM_s decreases by 11.6, 26.7, 67.4, and 19.3% and M_s by 15.7, 26.7, 64.6, and 22.4% for samples 1, 2, 3, and 4, respectively. This results in a change of only 4, 0, 3, and 3%, respectively, for R_s with T over this wide range of temperature. Thus to find the temperature dependence of R_s and ultimately to check the scaling relation $R_s \sim \rho^n$ becomes ex-
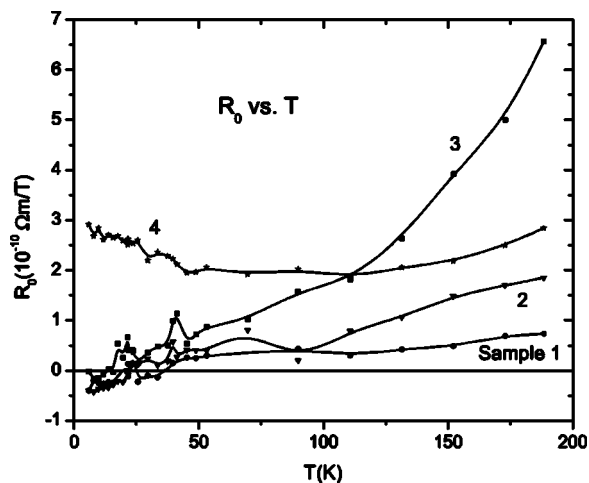

FIG. 2. The ordinary Hall constant R_0 vs temperature for all the samples showing a weak temperature dependence except for sample 3. The solid lines are just guides to the eye.
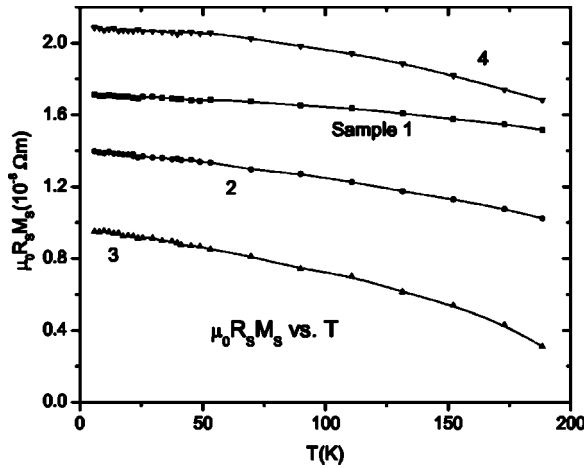
FIG. 3. $\mu_0 R_s M_s$ (intercept with the ρ_H axis of Fig. 1) vs temperature for all the samples showing a weak temperature dependence below 50 K. The solid lines are just guides to the eye.

FIG. 5. Electrical resistivity ρ vs temperature for all the samples. The points are the raw data, and the thick solid lines are the best fits of ρ to Eq. (6) at very low temperatures ($T \leqslant 22$ K).

tremely difficult, if not impossible for some of the present samples. This is because of the very similar decrease of $R_s M_s$ and M_s with temperature. For example in sample 2, R_s hardly changes (0%). For sample 3, although R_s apparently decreases by 3%, the accuracy of $R_s(T)$ is very poor since it is determined from the large decrease of $R_s M_s (67.4\%)$ and M_s (64.6%) with T due to its T_c of only 222 K. This decrease of 3% in R_s is not significant since the errors in $R_s M_s$ and M_s are at least 1% each.

The temperature dependence of the electrical resistivity (ρ) is shown in Fig. 5 for all the samples. The data for samples 1, 2, and 3 are taken every 1 K, and thus the curves look almost continuous. They show resistivity minima (T_m) at 15, 65, 35, and 24 K, respectively, for samples 1, 2 3, and 4. In the temperature range of 5–190 K (Fig. 5) ρ has a weak temperature dependence for samples 2 and 3 and somewhat stronger for 4 and 1. In order to correlate R_s with ρ we have plotted in Figs. 6 and 7 their (R_s and ρ) temperature depen-

dences on the same graph for the more favorable samples 1 and 4, respectively [which show meaningfully measurable $\approx (3-4)\%$ changes in $R_s(T)$]. It is amply clear from Fig. 6 that sample 4 shows a minimum in R_s at about 25 K, the same temperature at which the electrical resistivity shows a minimum. The large error bars in R_s are due to the similar decrease of $R_s M_s$ and M_s with T, as mentioned above. The minimum is not as clear in Fig. 7 (sample 1) but it cannot be overlooked. We must mention here that $R_s(T)$ has to be determined from two independent measurements, the Hall resistivity and the magnetization. Also, in ferromagnetic materials where $R_s M_s$ increases with temperature the extraction of $R_s(T)$ is much more accurate since M_s always decreases with temperature. A comparison of the absolute values of R_s in our samples (typically 3×10^{-8} Ωm/T) gives a reasonable agreement with the values obtained by Ivkov *et al.*[10] (typically 2×10^{-8} Ωm/T). Also, R_s increases from 2.4×10^{-8} to 4×10^{-8} Ωm/T from sample 2 to 3 which have similar com-
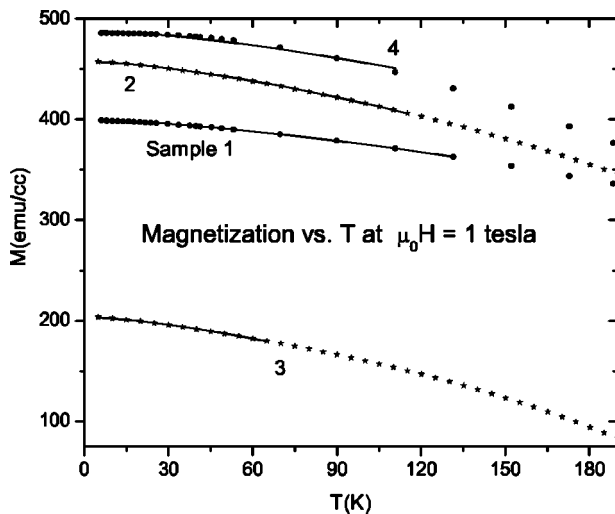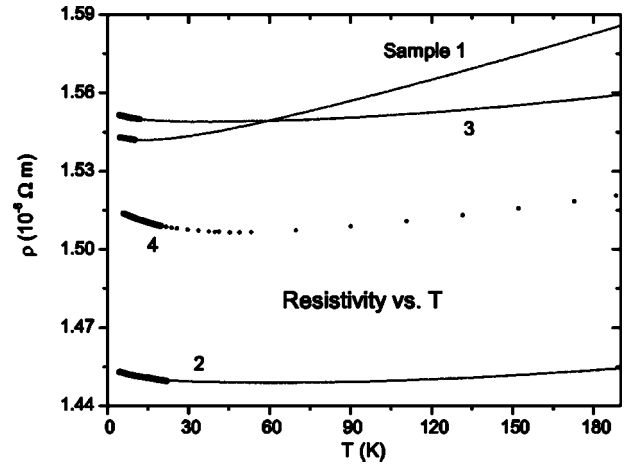

FIG. 4. Magnetization M vs temperature for all the samples at $\mu_0 H = 1$T. The solid lines are the best fits of M to Eq. (4) up to $T \simeq 0.3 T_c$.
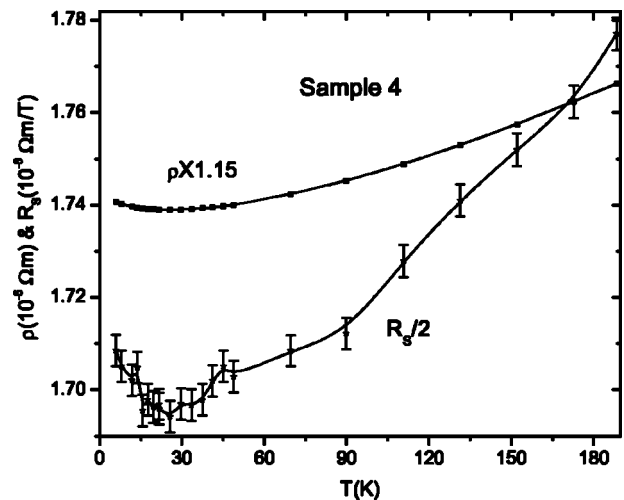

FIG. 6. R_s and ρ vs T for sample 4. Both show a minimum around 25 K. The error bars in R_s are also shown. The solid lines are just guides to the eye.
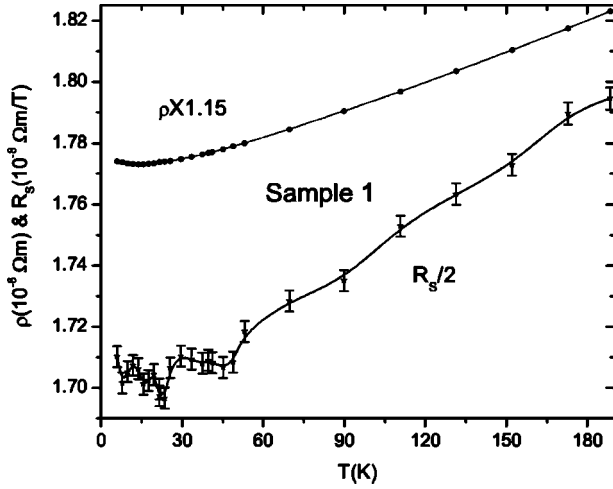
FIG. 7. The same as in Fig. 6 except that they are now for sample 1.

position but differ in Cr by only 5% at the cost of Ni. Since R_s in Ni is negative,[1] less Ni makes R_s more positive in these Co-rich ($R_s > 0$) metallic glasses.

To summarize, Figs. 6 and 7 clearly show that R_s and ρ go hand in hand. To the best of our knowledge there is no theoretical work on the effect of the electron-electron interaction on the side-jump mechanism or any other quantum transport theory for R_s. The coincidence of the minima only implies that the competing mechanisms responsible for the resistivity minima (viz., ρ decreasing with temperature due to *e-e* interaction and increasing with temperature due to electron-phonon scattering) also guide the temperature dependence of R_s through ρ. For samples 2 and 3, there is negligible temperature dependence of R_s, and no correlation with ρ, which also shows a very weak temperature dependence. To find the exponent n of $R_s \sim \rho^n$ we have plotted in Fig. 8 ln R_s vs ln ρ for both samples 1 and 4. The slope gives $n = 2.2 \pm 0.1$. In these high resistivity ($\sim 150~\mu\Omega$ cm) metal-
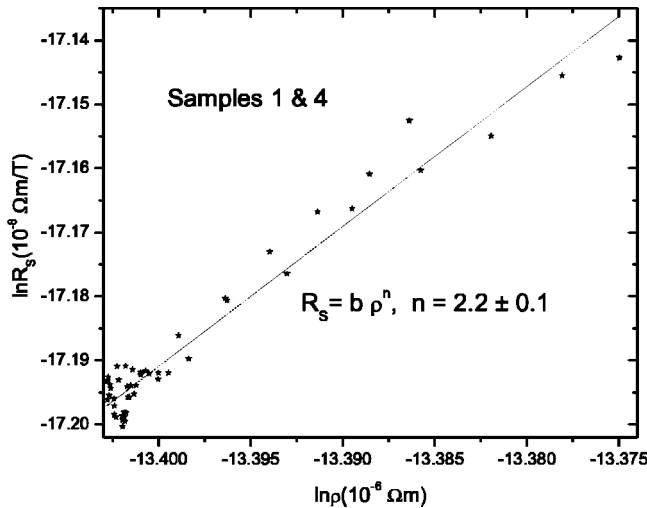

FIG. 8. ln R_s vs ln ρ for samples 1 and 4 on the same plot. The straight line is the best fit to the equation $R_s = b\rho^n$ with $n = 2.2 \pm 0.1$.

lic glasses nonclassical transport clearly dominates over the Smit asymmetric scattering[5] for which $n = 1$.

B. Magnetization

The good quality of magnetization data (Fig. 4) permits analysis of the process of thermal demagnetization in these metallic glasses. In both crystalline and amorphous ferromagnets, consideration of only the harmonic term in the spin-wave dispersion relation gives the following expression for the magnetization:[11,12]

$$M(T) = M(0)[1 + AT^{3/2}]. \quad (4)$$

Many amorphous ferromagnets follow Eq. (4) till $T \cong 0.3 T_c$.[13]

The spin-wave stiffness constant is related to A above and is given by

$$D = \frac{k_B}{4\pi}\left(\frac{2.612~g\mu B}{M(0)A}\right)^{2/3}. \quad (5)$$

The $M(T)$ data (Fig. 4) have been fitted to Eq. (4) up to $T \cong 0.3~T_c$. The solid lines in Fig. 5 represent the best fits to Eq. (4). These fits are quite good with correlation coefficients $\cong 0.999$ and χ^2 consistent with the experimental resolution. The spin-wave stiffness constants, calculated from Eq. (5), are found to be 108.6, 75.8, 71.2, and 89.9 meV Å^2 for samples 1, 2, 3, and 4, respectively. These values are comparable to the value 100 meV Å^2 found in many Fe-B metallic glasses.[14] $M(0)$ in samples 2 and 3 (which are very similar in composition but there is 5% more Cr in sample 3) are 460 and 200 emu/cc, respectively. Cr-Cr interaction in the localized model is antiferromagnetic and hence just 5% more Cr in sample 3 understandably reduces $M(0)$ considerably by a factor of ~ 2. A similar interesting consequence of antiferromagnetism of Cr is the reduction in T_c from 386 to 222 K.

C. Electrical resistivity

The relative accuracy of the electrical resistivity data shown in Fig. 5 is 10 ppm. Their values vary between 145 and 155 $\mu\Omega$ cm and have no significant composition dependence except that an additional 5% Cr in sample 3 (over sample 2) increases ρ from 145 to 155 $\mu\Omega$ cm. Cr increases ρ significantly also in crystalline NiCr binary alloys.[13] Many of the metallic glasses which have large electrical resistivity show minima in their temperature dependence similar to those shown in Fig. 5. They can be explained by quantum interference effects.[15,16] The equation

$$\rho(T) = \rho_0 - AT^{1/2} \quad (6)$$

describes this resistivity data very well below T_m with $A = (400-1000)\Omega$m K$^{-1/2}$ in agreement with many other metallic glass samples.[17,18] The thick solid lines in Fig. 5 are the best fits to Eq. (6) and yield correlation coefficients of $\cong 0.99$. Electron-electron interaction effects, in the presence of weak localization, predict $\rho \sim \sqrt{T}$ well below T_m. Thus the fits extended only to 12, 22, 10, and 20 K, respectively, for samples 1, 2, 3, and 4.

IV. CONCLUSIONS

The minima in the electrical resistivity and the extraordinary Hall effect go hand in hand in two of the ferromagnetic metallic glasses having a high resistivity $\simeq 150$ $\mu\Omega$ cm. In the other two samples the variation of R_s with temperature is comparable to its error. This is due to the fact that $R_s M_s$ and M_s have very similar decreases with increasing temperature. The temperature dependence of magnetization is well described by Bloch's $T^{3/2}$ law giving reasonable values of spin-wave stiffness constants. The resistivity minima are explained in terms of electron-electron interaction in the presence of weak localization as observed in many disordered systems.

*Author to whom correspondence should be addressed. Electronic address: akm@iitk.ac.in

[1] L. Berger and G. Bergmann, in *Hall Effect and its applications*, edited by C. L. Chien and C. R. Westgate (Plenum, New York, 1980), p. 55, and references therein.

[2] R. Karplus and J. M. Luttinger, Phys. Rev. **95**, 1154 (1954).

[3] J. M. Luttinger, Phys. Rev. **112**, 739 (1958).

[4] L. Berger, Phys. Rev. B **2**, 4559 (1970).

[5] J. Smit, Physica (Amsterdam) **21**, 877 (1955); **24**, 39 (1958).

[6] T. R. McGuire, R. J. Gambino, and R. C. O'handley, in Ref. 1, p. 137.

[7] T. Egami, Rep. Prog. Phys. **47**, 1601 (1984).

[8] H. K. Lachowicz, Phys. Status Solidi A **67**, K131 (1981).

[9] K. Shiba, S. Tsunashima, S. Uchiyama, and S. Yoshino, IEEE Trans. Magn. **22**, 1986 (1986).

[10] J. Ivkov, E. Babic, and Z. Markovic, J. Phys. Colloq. **49**, 1301 (1988).

[11] F. Keffer, in *Handbuch der Physik*, edited by S. Flűgge and H. P. J. Wijn (Springer, Berlin, 1966), Vol. XVIII/2, p. 1.

[12] U. Krey, Z. Phys. B **31**, 247 (1978).

[13] F. E. Luborsky, in *Ferromagnetic Materials*, edited by E. P. Wohlfarth (North-Holland, Amsterdam, 1980), Vol. 1, p. 497.

[14] A. K. Majumdar, V. Oestreich, D. Weschenfelder, and F. E. Luborsky, Phys. Rev. B **27**, 5618 (1983).

[15] P. A. Lee and T. V. Ramakrishnan, Rev. Mod. Phys. **57**, 287 (1985).

[16] J. S. Dugdale, Contemp. Phys. **28**, 547 (1987).

[17] R. W. Cochrane and J. O. Strom-Olsen, Phys. Rev. B **29**, 1088 (1984).

[18] T. K. Nath and A. K. Majumdar, Phys. Rev. B **55**, 5554 (1997).